Identification of Monosialylated *N*-glycoforms in the CDG Urinome by Ion Mobility Tandem Mass Spectrometry: The Potential for Clinical Applications

Sergey Y. Vakhrushev · James Langridge · Iain Campuzano · Chris Hughes · Jasna Peter-Katalinić

Abstract

Introduction A novel approach of ion mobility tandem mass spectrometry (IMS-MS/MS) is applied to analysis of human glycourinome to obtain carbohydrate pattern data of congenital disorders of glycosylation patient. Overlapping of the complex carbohydrate mass range landscape has been highly reduced upon IMS-MS procedure, allowing more efficient identification by mapping and sequencing of glycan precursor ions, following their separation by mobility, according to difference in drift time through the traveling wave IMS cell. Intact and truncated N- and O-glycan structures modified by sialylation and fucosylation were identified according to their drift time separated molecular ions and submitted to fragmentation in a narrow mass window.

IMS CID MS/MS Analysis The fragmentation spectra generated from the IMS separated precursor ions contain series of fragment ions maintaining the same mobility as their parent ions, and the assignment accuracy can be significantly enhanced.

Conclusion According to the specific fragment ion patterns, carbohydrate epitopes described to be involved in pathological processes were assigned. A high potential of this glycomics-based strategy for clinical applications can be presented.

S. Y. Vakhrushev · J. Peter-Katalinić (✉)
Institute for Medical Physics and Biophysics,
Biomedical Analysis Department, University of Münster,
Robert-Koch-Str. 31,
48149 Muenster, Germany
e-mail: jkp@uni-muenster.de

J. Langridge · I. Campuzano · C. Hughes
Waters Corporation,
Atlas Park, Simonsway,
Manchester M22 5PP, UK

Introduction

Congenital disorders of glycosylation (CDG) are a large family of genetic diseases resulting from defects in the synthesis of glycans and in the attachment of glycans to lipids and proteins. These disorders cause a wide range of clinically relevant human diseases with different, sometimes diffuse, clinical pictures. There are currently 12 defined N-, seven O- and three N- and O-glycosylation defects due to defects in proteins with glycosyltransferase or transport function already identified [1]. For a growing group of patients with unidentified defects, but typical and atypical clinical presentations in CDG, there is a high need for an increase in the speed and accuracy of diagnostics in order to design rational therapeutic suggestions in as short a time span as possible.

The alteration of glycan patterns related to CDG defects is reflected in the patients' serum, which can be analyzed for glycosylation patterns of glycoproteins, according to proteomics-based protocols [2]. However, urine as a rich source of metabolic structures renders an excellent opportunity for noninvasive sample diagnostics. Carbohydrate patterns of CDG patients' urine were investigated by us using distinct glycomics-based strategies to explore the feasibility of protocols and their potential for unique structure discovery and clinical applications [3–6]. Components of these highly complex mixtures depict different levels of modifications by sialylation and fucosylation. A high number of intact and truncated N- and O-glycan structures were revealed by high resolution mass spectrometry and correlated to the structures deposited in the

databases [4]. Using a novel approach of ion mobility mass spectrometry (IMS-MS), overlapping of the carbohydrate mass range landscape was shown to be highly reduced, allowing development of strategies for more efficient identification by sequencing the glycan precursor ions, following their separation by their mobility, or drift time, through the traveling wave IMS cell [3]. The fragmentation data obtained clearly demonstrate that carbohydrate epitopes can be de novo identified by this type of bioanalysis rendering an efficient novel tool for glycomics to be introduced to the CDG research and be applied to clinical samples. In the following investigation, monosialylated glycoforms from urine and their terminal epitopes were identified by IMS and automatic data assignment to be correlated with those described in carbohydrate databases for comparison of their possible function.

Materials and Methods

Materials and Sample Preparation

Materials Methanol was obtained from Merck (Darmstadt, Germany) and used without further purification. Graphitized carbon powder for the graphitized carbon cartridge preparation was collected by dismantling commercially available Active Charcoal MicroTip Columns 25-100 µl (Harvard Apparatus Inc). AG50 (H^+) resin was purchased from Bio-Rad (Richmond, CA, USA). Distilled and deionized water (Mili-Q water systems Millipore, Bedford, MA, USA) was used for the preparation of the sample solutions.

CDG urine sample The sample investigated in this study was a native glycoconjugate mixture from the urine of patient K.L. suffering from symptoms assigned to the congenital disorder of glycosylation (CDG). For isolation of components, the patient's urine was filtered and submitted to a first gel filtration chromatography step on Biogel P2 followed by several chromatography stages as described previously [4, 5]. The fraction M3 from the patient K.L. was used in the present study.

Desalting of glycoconjugate mixtures Prior to analysis by mass spectrometry, the fraction M3 containing a mixture of glycoconjugates was purified by homemade graphitized carbon cartridges as described previously [7] and desalted by AG50 (H^+) resin.

Mass spectrometry All measurements were performed on a Synapt high-definition mass spectrometry (HDMS) system (Waters, Manchester, UK). The Synapt HDMS is a hybrid

quadrupole-triwave IMS-oa-TOF device. Gas-phase ions were generated by nano-electrospray ionization in the negative ion mode, passed through a quadrupole into the triwave cell where the ions were separated according to their mobility, and finally transferred to the oa-TOF mass analyzer [3]. Ion source conditions were optimized to minimize in-source fragmentation. DriftScope™ Mobility Environment software was used for ion mobility data visualization and manipulation. Instrumental control and mass spectra acquisition were operated by Waters MassLynx 4.1 software.

Collision-induced dissociation (CID) structural analysis of selected ionic species was performed by transfer T-Wave fragmentation [3]. The fragmentation pattern of sequenced glycoconjugates was assigned according to nomenclature introduced by Domon and Costello [8].

Data interpretation The computer algorithm for mass spectrometry data interpretation was developed by using Borland Delphi 7 for Windows (Borland) [3]. All computational assignments have been performed within the mass accuracy range of 0–25 ppm.

Glycan database Consortium for Functional Glycomics (http://www.functionalglycomics.org, 2008) and Glycosuite DB (https://tmat.proteomesystems.com/glycosuite, 2004) glycan databases has been used for correlation with proposed compositions by searching of structural information, such as the type and the number of monosaccharide building blocks. The list of previously described oligosaccharide structures related to the imported composition was generated as the output, providing information about the sample source, methods of structural elucidation, and the corresponding references.

Results

IMS-MS Glycoscreening of the KLM3 CDG Sample

Mapping and sequencing of monosialylated free and amino acid-linked glycans in the urine of the CDG patient K.L. has been probed in the fraction KLM3 to identify the type of glycans involved, their branching patterns, and sialylation attachment. Analyzed in the negative ion MS mode using a nanoESI oa-TOF mass spectrometer more than 100 singly, doubly, and triply charged ions has been observed (Fig. 1). Three ubiquitous singly charged ion species at m/z 632.21, 673.22, and 876.30 assigned previously to NeuAcHex$_2$, NeuAcHexHexNAc, and NeuAcHexHexNAc$_2$, respectively, were present at high abundance 40–100%, but the majority of the ionic species, with highly over-

Fig. 1 Negative ion mode nanoESI oa-TOF MS of the fraction M3 obtained from urine of the patient KL after gel permeation chromatography. Spectrum was acquired from the TIC chromatogram over all mobility drift times. *Inset*: plot of the drift time vs. *m/z* values for the negative ion mode nanoESI oa-IMS-TOF MS. Ions have been distributed onto areas of predominantly singly (*A*), doubly (*B*), and triply (*C*) charged ionic species (selected by *dashed lines*). XIC chromatograms *A*, *B*, and *C* were generated from the corresponding area
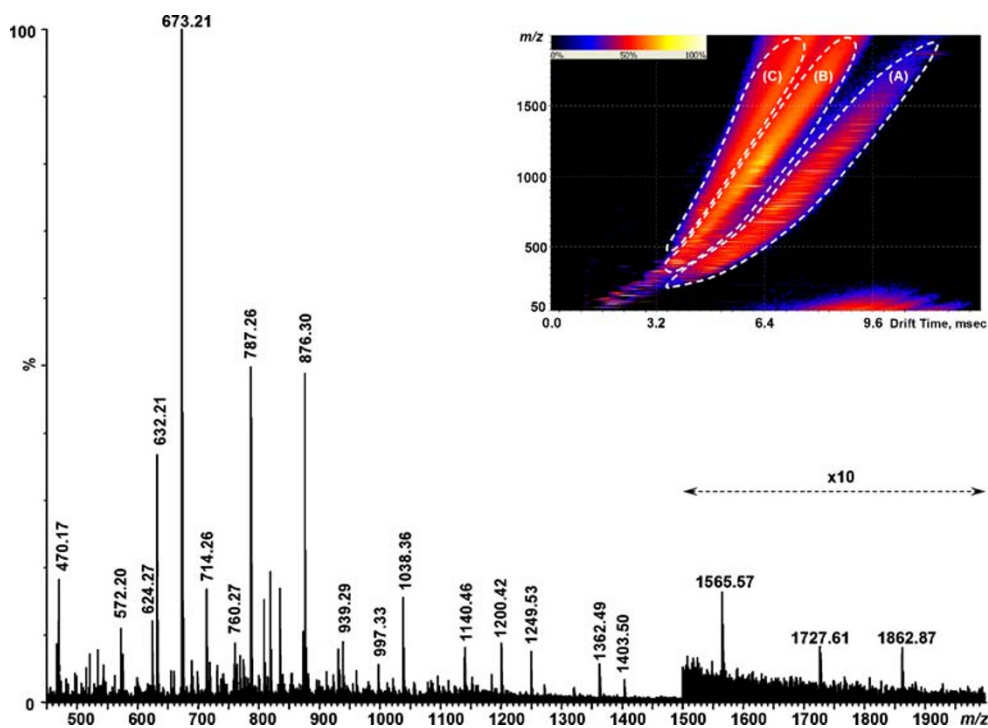
lapping isotopic envelopes, were at or below 15%, substantially hindering the tandem MS identification by mapping and sequencing. As already reported, the introduction of IMS as an additional dimension prior to mass analysis allows effective separation of molecular ions in the gas phase according to their charge, shape, and size [3]. Briefly, the ions are separated by their mobility through the dense gas-filled traveling wave and, subsequently, mass analyzed by the oa-TOF. Plotting the ions drift time versus their *m/z* values, it can be observed that the signal is distributed into three distinct nested areas, A, B, and C, based upon their *m/z* and drift time relationship. These nested sets correspond to the singly, doubly, and triply charge ions, respectively (Fig. 1, inset). Selection of these regions and maintaining their *m/z* and drift times produce mass spectra containing predominantly singly, doubly, and triply charged ion populations. These ions previously overlapped in the TOF MS acquisition are now separated and localized into the regions A, B, and C (Fig. 2). The ions with the signal-to-noise ratio significant for the determination of isotopic distribution are selected and submitted for automated compositional analysis calculation.

The singly charged ion population obtained by selecting region A (Fig. 1a) exposed the presence of at least 62 distinct ionic species, mostly below 15% abundance. Close inspection of the mass spectrum acquired upon IMS separation revealed a significant improvement in the signal-to-noise ratio, as illustrated for the mass range 1500–2000 Da. The data that acquired overall mobility drift times show only three ions at *m/z* 1565.57, 1727.60,

and 1862.88 (Fig. 1), where in the same *m/z* range of the singly charged spectrum acquired from region A, six additional species at *m/z* 1548.70, 1768.64, 1846.84, 1878.82, 1884.87, and 1930.65, respectively, can be easily detected (Fig. 2a). Consideration of the established N-glycan biosynthetic pathways allows the composition of ions at *m/z* 1565.70, 1727.60, 1768.64, and 1930.65 to be assigned as $[NeuAcHex_4HexNAc_3-H]^-$, $[NeuAcHex_5HexNAc_3-H]^-$, $[NeuAcHex_4HexNAc_4-H]^-$, and $[NeuAcHex_5HexNAc_4-H]^-$, respectively and proposed to represent free N-glycans without Asn attachment at the reducing end. Computational analysis of all singly charged species in the region A ion population allowed the compositions of ~67% of the selected ions to be accomplished. The majority of the species were proposed to represent free oligosaccharides, except 11 ionic species identified by calculation as O-glycans linked either to Ser, Thr, ThrPro, or SerThr (Table 1).

All doubly charged ions obtained by averaging over region B were low abundant at the level of relative intensity below ~12% (Fig. 2b). According to the compositional analysis, 15 species out of 58 were assigned to free oligosaccharides (Table 1). Three doubly charged ions at *m/z* 758.25, 839.29, and 1094.86 were proposed to represent N-glycans linked to Asn and assigned as $[NeuAcHex_3HexNAc_3Asn-2H]^{2-}$, $[NeuAcHex_4HexNAc_3Asn-2H]^{2-}$, and $[NeuAcdHexHex_5HexNAc_4Asn-2H]^{2-}$, respectively. Four doubly charged O-glycan species were proposed according to the compositional analysis to be linked at their respective reducing termini to Thr, Ser, Ser-Thr, or Thr-Pro. These are the ionic species detected at *m/z*

Fig. 2 Negative ion mode nanoESI oa-IMS-TOF MS of the sample KLM3 acquired over: **a** XIC chromatogram A, **b** XIC chromatogram B, and **c** XIC chromatogram C (Fig. 1, *Inset*)
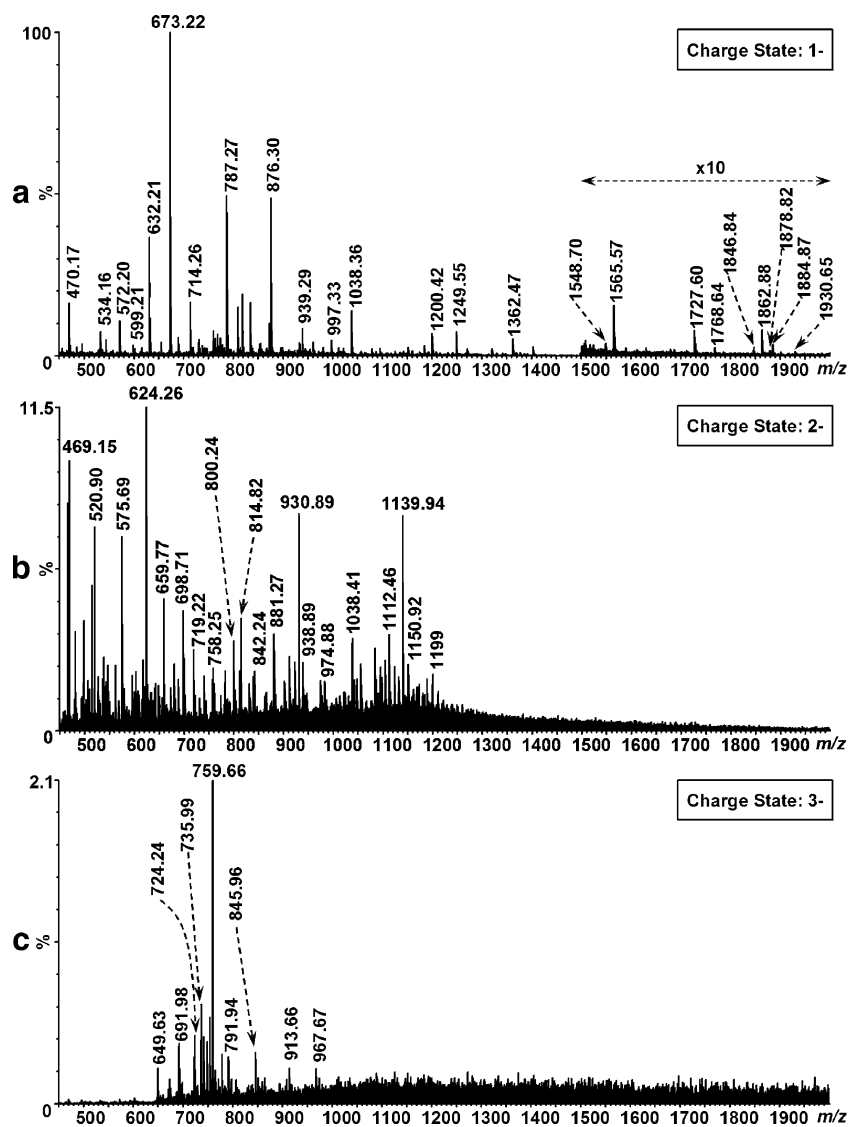
436.16, 562.19, 575.69, and 974.88 assigned to [dHexHexNAc₃Thr-2H]$^{2-}$, [NeuAcHex₂HexNAc₂Ser-2H]$^{2-}$, [NeuAc₂HexHexNAcSerThr-2H]$^{2-}$, and [NeuAcdHexHex₃ HexNAc₄ThrPro-2H]$^{2-}$, respectively. In the doubly charged pool, the ions detected in the abundance range of 8–12% at m/z 469.15, 624.26, 930.89, and 1139.94 could not be assigned to any glycoconjugate structures; but, according to their CID MS/MS data, they could be assigned as collagen peptides containing a common Gly-Leu/Ile-Pro repeat (data not shown).

The data from region C produced 18 triply charged species with distinct isotopic distribution that were utilized for compositional analysis (Fig. 2c) and showed only six ionic species representing glycoconjugates (Table 1). Ionic species at m/z 675.57 and 797.27 were assigned to [NeuAcdHexHex₄HexNAc₄Asn-3H]$^{3-}$ and [NeuAcdHex Hex₅HexNAc₅Asn-3H]$^{3-}$, respectively. On the other hand,

triply charged ions at m/z 791.94, 845.96, 913.66, and 967.67 could be simultaneously assigned to free oligosaccharides such as [NeuAcHex₄HexNAc₇–3H]$^{3-}$, [NeuAc Hex₅HexNAc₇–3H]$^{3-}$, [NeuAcHex₅HexNAc₈–3H]$^{3-}$, [NeuAcHex₆HexNAc₈–3H]$^{3-}$, or Asn-linked N-glycans, such as [NeuAcdHex₂Hex₄HexNAc₅Asn-3H]$^{3-}$, [NeuAc dHex₂Hex₅HexNAc₅Asn-3H]$^{3-}$, [NeuAcdHex₂Hex₅HexN Ac₆Asn-3H]$^{3-}$, and [NeuAcdHex₂Hex₆HexNAc₆Asn-3H]$^{3-}$, respectively (Table 1). The most intensive triply charged ions detected at m/z 759.66 below 2% abundance were assigned to a collagen peptide with Gly-Leu/Ile-Pro repeat (data not shown).

Thus, in total 138 ionic species with distinct isotopic distribution have been detected by IMS oa-TOF MS approach, and 47 singly and multiply charged species that previously overlapped became well separated using this approach.

Table 1 Computer-assisted assignment of the major peaks detected in KLM3 sample by the negative ion nanoESI IMS oa-TOF MS

No.	[M-H]-	[M-2H]2-	[M-3H]3-	Proposed Composition	MW[f]	References[g]
1	496.18			HexHexNAcAsn	497.19	–
2	544.20			$Hex_2HexNAc$	545.20	i
3	602.21[a]			HexHexNAcThrPro	581.24	–
4	599.21			$NeuAc_2$	600.20	–
5	632.21			$NeuAcHex_2$	633.21	[16, 17]
6	655.23[b]			NeuAcHexHexNAc	674.24	[16–23]
	673.22					
7	714.26			$NeuAcHexNAc_2$	715.27	i
8	769.26[a]			$Hex_2HexNAc_2$	748.27	[24, 25]
9	760.27			NeuAcHexHexNAcSer	761.27	[26–28]
	764.25[c]					
10	774.29			NeuAcHexHexNAcThr	775.29	[26–28]
	778.26[c]					
11	809.25[b]			Hex_5	828.27	–
12	819.29			NeuAcdHexHexHexNAc	820.30	h
13	835.29			$NeuAcHex_2HexNAc$	836.29	[29]
14	873.34	436.16		$dHexHexNAc_3Thr$	874.35	–
15	876.30			$NeuAcHexHexNAc_2$	877.32	[19, 30]
16		481.66		$NeuAc_2HexHexNAc$	965.33	[16, 19–23, 26–28, 31, 32]
17	981.34			$NeuAcdHexHex_2HexNAc$	982.35	i
18	997.33			$NeuAcHex_3HexNAc$	998.34	i
19	1038.36			$NeuAcHex_2HexNAc_2$	1039.37	[19, 22, 33]
20	1079.39			$NeuAcHexHexNAc_3$	1080.40	i
21	1125.38	562.19		$NeuAcHex_2HexNAc_2Ser$	1126.40	–
22	1143.38			$NeuAcdHexHex_3HexNAc$	1144.40	–
23	1152.41	575.69		$NeuAc_2HexHexNAcSerThr$	1153.41	–
24	1184.42	609.68[d]		$NeuAcdHexHex_2HexNAc_2$	1185.43	i
25	1200.42	617.69[d]		$NeuAcHex_3HexNAc_2$	1201.42	[10, 17]
26	1241.45			$NeuAcHex_2HexNAc_3$	1242.45	i
27	1362.47	680.72		$NeuAcHex_4HexNAc_2$	1363.48	[10, 11]
		698.71[d]				
28	1369.49[b]			$NeuAcdHexHex_2HexNAc_3(-H_2O)$	1388.51	i
29	1403.49	719.22[d]		$NeuAcHex_3HexNAc_3$	1404.50	i
30		744.75[b]		$NeuAcdHexHex_4HexNAc_2$	1509.53	–
31		758.25		$NeuAcHex_3HexNAc_3Asn$	1518.54	–
32	1565.57	800.24[d]		$NeuAcHex_4HexNAc_3$	1566.55	[10, 34, 35]
33		803.76[e]		$NeuAcdHexHex_2HexNAc_4$	1591.59	–
		812.75[d]				
34		839.29		$NeuAcHex_4HexNAc_3Asn$	1680.60	–
35	1727.60	881.27[d]		$NeuAcHex_5HexNAc_3$	1728.61	[10, 11, 34, 35]
36	1768.64			$NeuAcHex_4HexNAc_4$	1769.63	h
37	1930.65	982.81[d]		$NeuAcHex_5HexNAc_4$	1931.69	[13, 34, 36]
38		974.88		$NeuAcdHexHex_3HexNAc_4ThrPro$	1951.74	–
39			675.57	$NeuAcdHexHex_4HexNAc_4Asn$	2029.74	–
40		1055.85[d]		$NeuAcdHexHex_5HexNAc_4$	2077.74	[13, 36]
41		1094.86		$NeuAcdHexHex_5HexNAc_4Asn$	2191.79	–
42		1150.92		$NeuAcdHexHex_4HexNAc_6$	2303.84	–
43			791.94	$NeuAcHex_4HexNAc_7$	2378.87	–
				$NeuAcdHex_2Hex_4HexNAc_5Asn$	2378.87	–
44			797.27	$NeuAcdHexHex_5HexNAc_5Asn$	2394.87	–
45		1199.93		$NeuAcdHexHex_7HexNAc_4$	2401.85	–
46			845.96	$NeuAcHex_5HexNAc_7$	2540.93	–
				$NeuAcdHex_2Hex_5HexNAc_5Asn$	2540.93	–
47			913.66	$NeuAcHex_5HexNAc_8$	2744.00	–
				$NeuAcdHex_2Hex_5HexNAc_6Asn$	2744.00	–

Table 1 (continued)

No.	[M-H]-	[M-2H]2-	[M-3H]3-	Proposed Composition	MW[f]	References[g]
48			967.67	NeuAcHex$_6$HexNAc$_8$	2906.06	–
				NeuAcdHex$_2$Hex$_6$HexNAc$_6$Asn	2906.06	–

[a] [M-2H+Na]⁻

[b] [M(-H$_2$O)-H]⁻

[c] [M(-H$_2$O)-2H+Na]⁻

[d] [M-H+Cl]²⁻

[e] [M(-H$_2$O)-H+Cl]²⁻

[f] Calculated molecular weight of the proposed composition.

[g] References are related to glycoconjugates previously found in *Homo sapiens* urine as free molecular species or as glycans obtained by protein deglycosylation.

[h] Glycoconjugates found in different organs from *Homo sapiens* urogenital system, besides urine.

[i] Glycoconjugates found in *Homo sapiens* from systems other than urogenital.

IMS CID MS/MS Analysis

For the investigation of glycan structure by tandem MS analysis, the overlapping of precursor ions represents a significant obstacle since a mixture of fragment ions originating from ions at the same or similar *m/z* values does not deliver useful data for assignment. In the case of overlapping ion envelopes of the singly charged species at *m/z* 1200.42 and the doubly charged at *m/z* 1199.93 assigned to [NeuAcHex$_3$HexNAc$_2$-H]⁻ and [NeuAcdHex-Hex$_7$HexNAc$_4$–2H]²⁻, respectively, the isotopic pattern of the doubly charged ions is obscured by that of the singly charged one (Fig. 3a), obstructing both the determination of the monoisotopic *m/z* value and selection of the appropriate
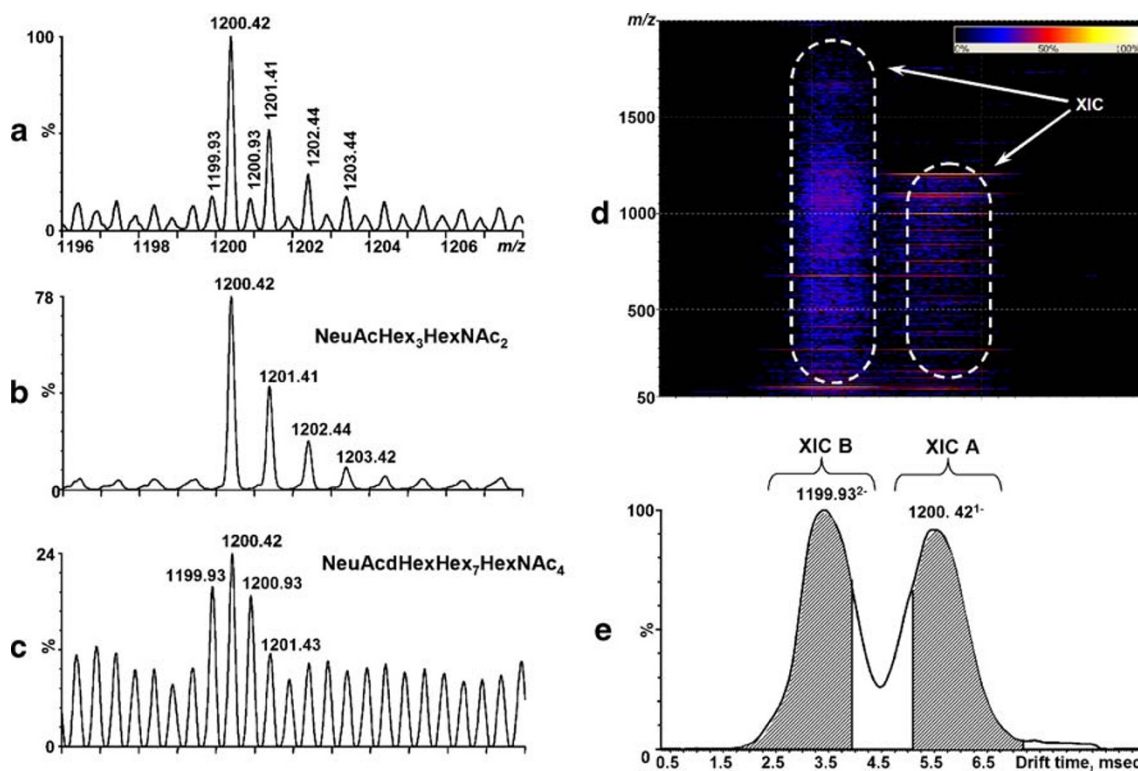
Fig. 3 **a** Expansion of the mass range at *m/z* 1196–1208 of the negative ion mode nanoESI oa-TOF MS of the fraction KLM3, acquired from TIC chromatogram over all mobility drift times; **b** expansion of the mass range at *m/z* 1196–1208 of the spectrum acquired from XIC chromatogram of singly charged distributed area after IM separation; **c** Expansion of the mass range at *m/z* 1196–1208 of the spectrum acquired from XIC chromatogram of doubly charged distributed area after IM separation; **d** Plot of the drift time vs. *m/z* values for fragment ions obtained by CID of overlapped precursor ions at *m/z* 1199.93 (*left*) and 1200.42 (*right*); **e** Total ion current chromatogram with retained drift time of overlapped precursor ions at *m/z* 1199.93 (*left*) and 1200.42 (*right*). Selected areas indicate extracted ion current chromatogram A for the precursor ions at *m/z* 1200.42 and chromatogram B for the precursor ions at *m/z* 1199.93

ion selection for fragmentation. Upon separation of the overlapping precursor ions by ion mobility, CID fragmentation using a transfer traveling wave gas cell, which is located after the IMS gas cell, generates distinct sets of fragments, as illustrated for ions at m/z 1200.42 and 1199.93 (Fig. 3b and c). The CID fragmentation of these IMS separated precursor ions generates series of fragment ions maintaining the same mobility as their parent ions (Fig. 3d). These distinct drift time areas can be used to generate individual chromatograms and, subsequently, mass spectra (A and B, respectively), as shown in Fig. 3e.

The fragmentation spectrum representing the glycan sequence of the singly charged precursor ions at m/z 1200.42 assigned to $[\text{NeuAcHex}_3\text{HexNAc}_2\text{-H}]^-$ obtained from drift time region A (Fig. 3e) is presented in Fig. 4. According to the evidence of the $^{0,2}A_6$ cross-ring fragment ions at m/z 1099.36, the free HexNAc residue at the reducing end can be proposed [5]. The observed loss of $\Delta m = 131u$ and $161u$ from the parent ions allows assignment of m/z 1069.42 and m/z 1039.35 as $^{2,4}A_6$ and $^{0,3}A_6$ cross-ring fragment ions, respectively, and proposes further extension of the reducing end only at the "C4" position of the HexNAc. The loss of $\Delta m = 60u$, detected at m/z 937.32 from the C_5 fragment at m/z 997.32, indicates that the next structural element elongating the reducing HexNAc is the Hex and can be assigned to $^{0,2}A_5$ fragment ions. Further inspection of the spectrum revealed the presence of an ion series, indicating the existence of a NeuAcLacNAc motif in the structure. Ions at m/z 290.09, 452.14, 655.22, and 673.23 compositionally proposed as NeuAc($-\text{H}_2\text{O}$), NeuAcHex, NeuAcHexHexNAc($-\text{H}_2\text{O}$), and NeuAcHexHexNAc could be assigned to B_1, B_2, B_3, and C_3 glycosidic fragments. Taking into account the presence

of Z_2, Y_2, B_4, and C_4 at m/z 364.13, 382.14, 817.27, and 835.28, respectively, as well as the rules of glycan assembly, the potential structural candidate was proposed as a truncated sialylated N-glycan NeuAc(α2–6)Gal(β1–4)GlcNAc(β1–2)Man(α1–3/6)Man(β1–4)GlcNAc with only one antenna, where the α2–6 linkage between NeuAc and Gal was proposed according to the diagnostic $^{0,4}A_2$-CO_2 cross-ring fragment being present at m/z 306.12 [9]. Searching the glycan database (http://www.functionalgly comics.org, 2008; https://tmat.proteomesystems.com/glyco suite, 2004) allowed correlation of the proposed structure with the one previously found in the urine of a patient suffering from infantile sialidosis, type II (dysmorphic) [10, 11]. On the other hand, a number of ions which cannot originate from the proposed structure, such as NeuAcHexHexNAc$_2$ at m/z 876.35 or NeuAcHex$_2$ at m/z 632.21, were also found in the spectrum, indicating the existence of an additional structural isomer with the same composition.

The fragmentation pattern of the doubly charged precursor at m/z 1199.93 separated by IMS and obtained by selecting the data shown in region B (Fig. 3e) can be assigned to $[\text{NeuAcdHexHex}_7\text{HexNAc}_4\text{–2H}]^{2-}$ (Fig. 5a). Inspection of the MS/MS spectrum revealed the presence of fragment ions corresponding to NeuAc($-\text{H}_2\text{O}$) at m/z 290.10, NeuAcHex at m/z 470.17, and NeuAcHexHexNAc at m/z 673.26. Besides the NeuAcLacNAc antennae terminal, a NeuAcLe$^{a/x}$ antennae structure was present according to the presence of the fragment ion at m/z 819.35. Thus, taking into account the biosynthetic rules of N-glycan antennae assembly as well as the evidence of the existence of truncated glycans in the urine, the structure of this species has been proposed, as summarized in Fig. 5b.

Fig. 4 Fragmentation pattern of the singly charged precursor ions at m/z 1200.42. The spectrum was obtained by averaging over XIC chromatogram A (Fig. 3e) after IMS separation. Inset: proposed structure—truncated sialylated biantennary N-glycan
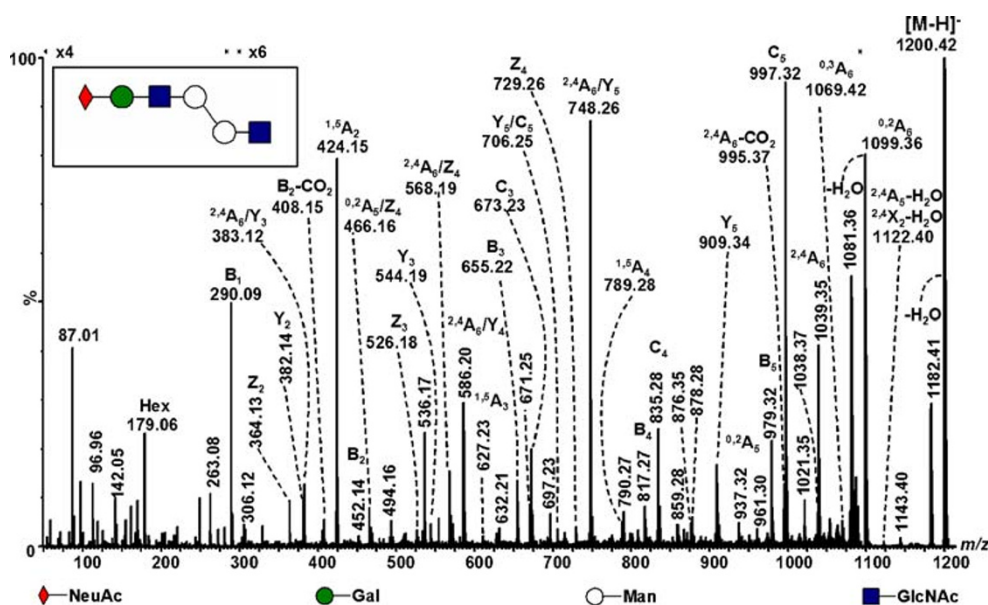
Fig. 5 a Negative ion mode nanoESI IMS oa-TOF MS/MS of the doubly charged precursor ions at m/z 1199.93. Fragmentation spectrum obtained by averaging over XIC chromatogram B (Fig. 3e) after IM separation. **b** Structural candidates proposed according to the rule of glycan biosynthesis and by the presence of diagnostic fragment ions
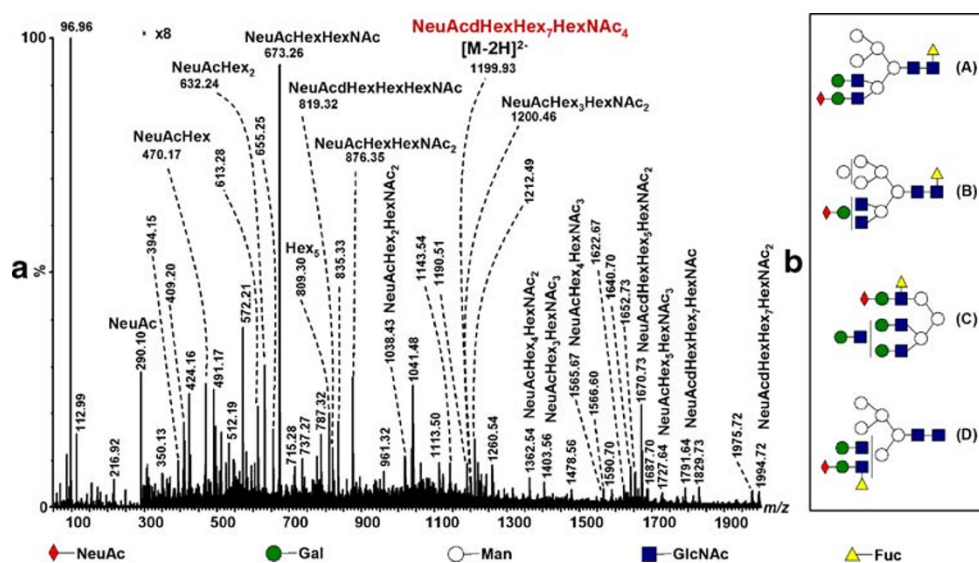
Ions at m/z 809.30 assigned to Hex_5(-H_2O) and m/z 1038.43 assigned to $NeuAcHex_2HexNAc_2$ were considered as "D" type and $C_{4\alpha}$ fragments, respectively, originating from the potential hybrid-type N-glycan isomer (Structure B, Fig. 5b). The double loss of a HexNAc unit from the parent ions detected at m/z 1994.72 indicates the absence of the core Fuc at the reducing end, and together with ions, indicating the presence of $NeuAcLe^{a/x}$ antennae can support structural isomer D (Fig. 5b). Ions at m/z 1143.54 assigned to $NeuAcdHexHex_2HexNAc$ can be considered as "D+H_2O" type fragment of the structural isomer, where the $NeuAcLe^{a/x}$ antennae is distributed at Man6 of the N-glycan core region (Structure C, Fig. 5b). Among the proposed structures depicted, only the structure A (Fig. 5b),

supported by the presence of $C_{4\alpha}$ at m/z 1200.46 has been found in the glycan database with a nonspecified source of origin (http://www.functionalglycomics.org, 2008).

The doubly charged precursor ions at m/z 1055.85 assigned to $[NeuAcdHexHex_5HexNAc_4-H+Cl]^{2-}$ represent another example of sialylated and fucosylated oligosaccharide found in the urine of CDG patient. To obtain a distinct series of fragment ions related only to the doubly charged precursors, IMS T-Wave transfer fragmentation analysis has been performed, and the spectrum acquired over the drift time range from 4.0 to 7.5 ms of the TIC chromatogram (Fig. 6a, inset). According to biosynthetic rules of glycan assembly and taking into account the ratio of monosaccharide units in the proposed composition, potential structural

Fig. 6 a Negative ion mode nanoESI IMS oa-TOF MS/MS of the doubly charged precursor ions at m/z 1055.85. Fragmentation spectrum obtained by averaging over XIC chromatogram (Inset, dashed line); **b** structural candidates proposed according to the rule of glycan biosynthesis and by the presence of diagnostic fragment ions
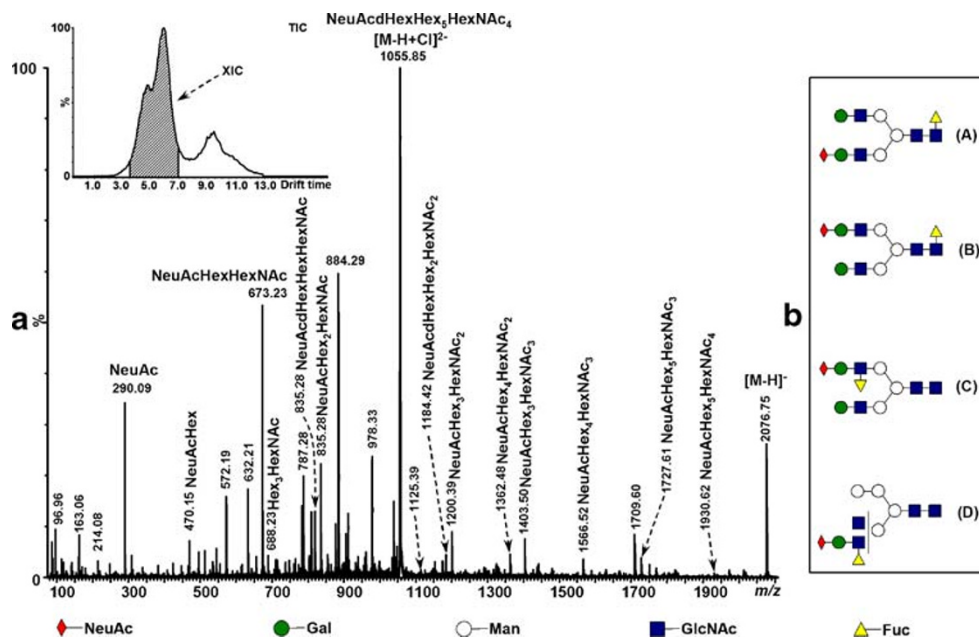
candidates could be proposed as monosialylated N-glycans with one peripheral or one core fucosylation. The presence of a NeuAcLacNAc antenna has been monitored by the diagnostic fragment ions assigned to NeuAcHexHexNAc detected at m/z 673.27. Fragment ions detected at m/z 819.29 and assigned to NeuAcHexHexNAc indicate a potential NeuAcLe[a/x] antennae structure, supporting the assumption of peripheral fucosylation. Thus, several structural isomers or isobars could be related to the precursor ions (Fig. 6b). The presence of diagnostic C_4 and "D" type fragment ions [12] allows to determine the distribution of antennae at the pentasaccharide core of potential structural candidates. Fragment ions at m/z 688.23 and 835.28 assigned to $Hex_2HexNAc$ and $NeuAcHex_2HexNAc$ has been considered as "D" and $C_{4\alpha}$, respectively, of the monosialylated biantennary N-glycan with core Fuc, where NeuAcLacNAc antenna is attached to Man3 of the core region (Structure A, Fig. 6b). The attachment of Neu

AcLacNAc antenna at Man6 of the core region has been specified by the presence of "D+H$_2$O" and $C_{4\beta}$ fragment ions at m/z 997.34 and 544.19, respectively (Structure B, Fig. 6b). On the other hand, fragment ions at m/z 544.19 can also be originated as $C_{4\beta}$ from the Structure C (Fig. 6b), supported by "D" and "D+H$_2$O" at m/z 1125.39 and 1143.39, respectively. The fourth structural candidate, isobaric with previous ones, could be proposed and assigned according to glycan biosynthesis rules to a hybrid type monosialylated N-glycan (Structure D, Fig. 6b). $C_{4\alpha}$ fragment ions detected at m/z 1184.42 and assigned to $NeuAcdHexHex_2Hex_2$ support this assumption. A correlation of the Structure A with that previously discovered in the urine of a male donor by monosaccharide analysis and ^{1}H NMR [13] has been done by glycan database search (http://www.functionalglycomics.org, 2008).

Thus, according to the analysis performed in this study, the present status of the KLM3 sample composition reveals

Table 2 Proposed structures carrying Sialyl T and Sialyl Le[a/x] associated epitopes found in KLM3 urinary sample

№	Proposed Structure [a]	Composition	MW [b]	Antigen
1		NeuAcHexHexNAc	674.24	Sialyl T
2		NeuAcHexHexNAc-Ser	761.28	Sialyl T
3		NeuAcHexHexNAc-Thr	775.29	Sialyl T
4		NeuAcdHexHexHexNAc	820.30	SiaLe[a/x]
5		$NeuAcdHexHex_2HexNAc_2$	1185.43	SiaLe[a/x]
6		$NeuAcdHexHex_5HexNAc_4$	2077.75	SiaLe[a/x]
7		$NeuAcdHexHex_5HexNAc_4$	2077.75	SiaLe[a/x]
8		$NeuAcdHexHex_7HexNAc_4$	2401.85	SiaLe[a/x]
9		$NeuAcdHexHex_7HexNAc_4$	2401.85	SiaLe[a/x]

[a] Symbolic presentation of glycoconjugate structures, where figures represent monosaccharides: ■ (GlcNAc), □ (GalNAc), ⊘ (Gal), ○ (Man), ◊ (NeuAc), △ (Fuc). Glycosidic linkages are schematically presented by differently oriented lines: — (1–4), / (1–3), \ (1–6) and | (1–2). For undefined type of glycosidic linkage dotted line was used.
[b] Calculated molecular weight of the proposed composition.

30 proposed structures which were found to be associated with detected ionic species. Upon classification of these 30 glycoconjugate structures, the expression of SiaLe$^{a/x}$ and Sialyl T terminal epitopes in both N- and O-linked glycan components could be postulated (Table 2). These epitopes have been previously observed in malignant tissues in different organs of human bodies, where glycosylation changes caused by cancer and/or inflammation diseases are the probable cause for their overexpression [14].

Since the significantly increased degree of core fucosylation of biantennary N-glycans as compared to normal has been reported in all so far known subtypes of CDG I [15], the validation of fucosylated oligosaccharides in the urine of CDG patient represents a potential direction for biomarker search.

Conclusions

Using the novel approach of ion mobility, separation coupled with tandem mass spectrometry intact and truncated N- and O-glycan structures from CDG patients' urine can be de novo identified by mapping and sequencing. By automatic assignment, the composition of single species from the IMS-separated spectra, with reduced complexity, were shown to be accessible for structure correlations to those in databases. Through the use of IMS, the overlapping carbohydrate m/z landscape was highly reduced in given window, allowing the development of a highly efficient identification procedure by sequencing precursor ions, using transfer CID fragmentation after separation by IMS. Combining it with a previously proposed automated calculation procedure provides an efficient novel tool for glycomics to be introduced, and this can readily be applied to CDG research and clinical samples. Accordingly, different levels of sialylation and fucosylation can be analyzed and assigned to truncated and untruncated glycan structures containing possible clinically relevant epitopes.

References

1. Jaeken J, Matthijs G. Congenital disorders of glycosylation: a rapidly expanding disease family. Annu Rev Genomics Hum Genet 2007;8:261–78.
2. Šagi D, Kienz P, Denecke J, Marquardt T, Peter-Katalinić J. Glycoproteomics of N-glycosylation by in-gel deglycosylation and matrix-assisted laser desorption/ionisation-time of flight mass spectrometry mapping: application to congenital disorders of glycosylation. Proteomics 2005;5:2689–701.
3. Vakhrushev SY, Langridge J, Campuzano I, Hughes C, Peter-Katalinić J. Ion mobility mass spectrometry analysis of human glycourinome. Anal Chem 2008;80:2506–13.
4. Vakhrushev SY, Mormann M, Peter-Katalinić J. Identification of glycoconjugates in the urine of a patient with congenital disorder of glycosylation by high-resolution mass spectrometry. Proteomics 2006;6:983–92.
5. Vakhrushev SY, Zamfir A, Peter-Katalinić J. $^{0,2}A_n$ cross-ring cleavage as a general diagnostic tool for glycan assignment in glycoconjugate mixtures. J Am Soc Mass Spectrom 2004;15:1863–8.
6. Zamfir A, Vakhrushev S, Sterling A, Niebel HJ, Allen M, Peter-Katalinić J. Fully automated chip-based mass spectrometry for complex carbohydrate system analysis. Anal Chem 2004;76:2046–54.
7. Packer NH, Lawson MA, Jardine DR, Redmond JW. A general approach to desalting oligosaccharides released from glycoproteins. Glycoconj J 1998;15:737–47.
8. Domon B, Costello CE. A systematic nomenclature for carbohydrate fragmentation in FAB MS/MS of glycoconjugates. Glycoconj J 1988;5:397–409.
9. Wheeler SF, Harvey DJ. Negative ion mass spectrometry of sialylated carbohydrates: discrimination of N-acetylneuraminic acid linkages by MALDI-TOF and ESI-TOF mass spectrometry. Anal Chem 2000;72:5027–39.
10. Nakamura Y, Takahashi Y, Yamaguchi S, et al. Severe infantile sialidosis–the characteristics of oligosaccharides isolated from the urine and the abdominal ascites. Tohoku J Exp.Med 1992;166:407–15.
11. Van Pelt J, Kamerling JP, Bakker HD, Vliegenthart JF. A comparative study of sialyloligosaccharides isolated from sialidosis and galactosialidosis urine. J Inherit Metab Dis 1991;14:730–40.
12. Šagi D, Peter-Katalinić J, Conradt HS, Nimtz M. Sequencing of tri- and tetraantennary N-glycans containing sialic acid by negative mode ESI QTOF tandem MS. J Am Soc Mass Spectrom 2002;13:1138–48.
13. Hard K, Van Zadelhoff G, Moonen P, Kamerling JP, Vliegenthart FG. The Asn-linked carbohydrate chains of human Tamm-Horsfall glycoprotein of one male. Novel sulfated and novel N-acetylgalactosamine-containing N-linked carbohydrate chains. Eur J Biochem 1992;209:895–915.
14. Dube DH, Bertozzi CR. Glycans in cancer and inflammation. Potential for therapeutics and diagnostics. Nat Rev Drug Discov 2005;4:477–88.
15. Callewaert N, Schollen E, Vanhecke A, Jaeken J, Matthijs G, Contreras R. Increased fucosylation and reduced branching of serum glycoprotein N-glycans in all known subtypes of congenital disorder of glycosylation I. Glycobiology 2003;13:367–75.
16. Parkkinen J, Finne J. Isolation and structural characterization of five major sialyloligosaccharides and a sialylglycopeptide from normal human urine. Eur J Biochem 1983;136:355–61.
17. Van Pelt J, Dorland L, Duran M, Hokke CH, Kamerling JP, Vliegenthart JF. Sialyl-alpha 2–6-mannosyl-beta 1–4-N-acetylglucosamine, a novel compound occurring in urine of patients with beta-mannosidosis. J Biol Chem 1990;265:19685–9.
18. Amano J, Nishimura R, Mochizuki M, Kobata A. Comparative study of the mucin-type sugar chains of human chorionic gonadotropin present in the urine of patients with trophoblastic diseases and healthy pregnant women. J Biol Chem 1988;263:1157–65.
19. Bhavanandan VP, Zhu Q, Yamakami K, et al. Purification and characterization of the MUC1 mucin-type glycoprotein, epitectin, from human urine: structures of the major oligosaccharide alditols. Glycoconj J 1998;15:37–49.
20. Gadroy P, Stridsberg M, Capon C, et al. Phosphorylation and O-glycosylation sites of human chromogranin A (CGA79–439) from urine of patients with carcinoid tumors. J Biol Chem 1998;273:34087–97.
21. Garver FA, Chang LS, Kiefer CR, et al. Localization of the carbohydrate units in a human immunoglobulin light chain, protein Sm lambda. Eur J Biochem 1981;115:643–52.

22. Irie F, Murakoshi H, Suzuki T, et al. Characterization of four monosialo and a novel disialo Asn N-glycosides from the urine of a patient with aspartylglycosaminuria. Glycoconj J 1995;12:290–7.

23. Van Pelt J, Van Bilsen DG, Kamerling JP, Vliegenthart JF. Structural analysis of O-glycosidic type of sialyloligosaccharide-alditols derived from urinary glycopeptides of a sialidosis patient. Eur J Biochem 1988;174:183–7.

24. Warner TG, Dekremer RD, Applegarth D, Mock AK. Diagnosis and characterization of GM2 gangliosidosis type-Ii (Sandhoff disease) by analysis of the accumulating N-acetyl-glucosaminyl oligosaccharides with high-performance liquid-chromatography. Clin Chim Acta 1986;154:151–64.

25. Strecker G, Herlantpeers MC, Fournet B, et al. Structure of seven oligosaccharides excreted in urine of a patient with sandhoffs disease (GM2 gangliosidosis-variant O). Eur J Biochem 1977; 81:165–71.

26. Frösch M, Bindila LM, Baykut G, Allen M, Peter-Katalinić J, Zamfir AD. Coupling of fully automated chip electrospray to Fourier transform ion cyclotron resonance mass spectrometry for high-performance glycoscreening and sequencing. Rapid Commun Mass Spectrom 2004;18:3084–92.

27. Zamfir A, Peter-Katalinić J. Glycoscreening by on-line sheathless capillary electrophoresis/electrospray ionization-quadrupole time of flight-tandem mass spectrometry. Electrophoresis 2001; 22:2448–57.

28. Hirabayashi Y, Matsumoto Y, Matsumoto M, et al. Isolation and characterization of major urinary amino acid O-glycosides and a dipeptide O-glycoside from a new lysosomal storage disorder (Kanzaki disease). Excessive excretion of serine- and threonine-linked glycan in the patient urine. J Biol Chem 1990;265:1693–701.

29. Pollitt RJ, Pretty KM. The glycoasparagines in urine of a patient with aspartylglycosaminuria. Biochem J 1974;141:141–6.

30. Escribano J, Lopex-Otin C, Hjerpe A, Grubb A, Mendez E. Location and characterization of the three carbohydrate prosthetic groups of human protein HC. FEBS Lett 1990;266:167–70.

31. Lecat D, Lemonnier M, Derappe C, et al. The structure of sialyl-glycopeptides of the O-glycosidic type, isolated from sialidosis (mucolipidosis I) urine. Eur J Biochem 1984;140:415–20.

32. Linden HU, Klein RA, Egge H, Peter-Katalinić J, Dabrowski J, Schindler D. Isolation and structural characterization of sialic-acid-containing glycopeptides of the O-glycosidic type from the urine of two patients with an hereditary deficiency in alpha-N-acetylgalactosaminidase activity. Biol Chem Hoppe Seyler 1989;370:661–72.

33. Amano J, Nishimura R, Sato S, Kobata A. Altered glycosylation of human chorionic gonadotropin decreases its hormonal activity as determined by cyclic-adenosine 3′,5′-monophosphate production in MA-10 cells. Glycobiology 1990;1:45–50.

34. de Beer T, van Zuylen CW, Hard K, et al. Rapid and simple approach for the NMR resonance assignment of the carbohydrate chains of an intact glycoprotein. Application of gradient-enhanced natural abundance 1H-13C HSQC and HSQC-TOCSY to the alpha-subunit of human chorionic gonadotropin. FEBS Lett 1994;348:1–6.

35. Weisshaar G, Hiyama J, Renwick AG. Site-specific N-glycosylation of human chorionic gonadotrophin–structural analysis of glycopeptides by one- and two-dimensional 1H NMR spectroscopy. Glycobiology 1991;1:393–404.

36. Nakano Y, Noda K, Endo T, Kobata A, Tomita M. Structural study on the glycosyl-phosphatidylinositol anchor and the asparagine-linked sugar chain of a soluble form of CD59 in human urine. Arch Biochem Biophys 1994;311:117–26.